Quality-Aware Fuzzy Min-Max Neural Networks for Dynamic Brain Network Analysis

Tao Hou, Jiashuang Huang, Shu Jiang, and Weiping Ding (✉)

School of Artificial Intelligence and Computer Science,
Nantong University, Nantong 226019, China
dwp9988@163.com

Abstract. Dynamic functional connections (dFCs) have been widely used for the diagnosis of brain diseases. However, current dynamic brain network analysis methods ignore the fuzzy information of the brain network and the uncertainty arising from the inconsistent data quality of different windows, providing unreliable integration for multiple windows. In this paper, we propose a dynamic brain network analysis method based on quality-aware fuzzy min-max neural networks (QFMM-Net). The individual window of dFCs is treated as a view, and we define three convolution filters to extract features from the brain network under the multi-view learning framework, thereby obtaining multi-view evidence for dFCs. We design multi-view fuzzy min-max neural networks (MFMM) based on fuzzy sets to deal with the fuzzy information of the brain network, which takes evidence as input patterns to generate hyperboxes and serves as the classification layer of each view. A quality-aware ensemble module is introduced to deal with uncertainty, which employs D-S theory to directly model the uncertainty and evaluate the dynamic quality-aware weighting of each view. Experiments on two real schizophrenia datasets demonstrate the effectiveness and advantages of our proposed method. Our codes are available at https://github.com/scurrytao/QFMMNet.

Keywords: Uncertainty · D-S theory · Dynamic brain network analysis.

1 Introduction

Dynamic functional connections (dFCs) are inferred from the time series of resting-state functional MRI (rs-fMRI), capturing the dynamic changes of activities in brain disease identification [13,15]. Recent studies have demonstrated the great promise of dFCs in understanding brain diseases by observing the temporal property changes and analyzing abnormal connections [5, 19]. Deep learning has excelled in discovering complex structures and learning latent features in high-dimensional data, showcasing the ability to explore intricate relationships and topological structures within dFCs. Therefore, brain network analysis algorithms based on deep learning have received growing attention [8, 16, 22].

However, current methods ignore the fuzzy information of the brain network and the uncertainty arising from the inconsistent data quality of different windows. Factors such as head motion, breathing, and heartbeat from the scanned volunteers impact the quality of data acquisition during the collection of raw rs-fMRI data, which leads to the generation of fuzzy information [1, 2]. Recent studies have concentrated on optimizing the preprocessing process, exhibiting a limited capability in dealing with fuzzy information, resulting in its widespread presence in dFCs [3, 4]. In addition, the traditional deep learning methods for dynamic brain network analysis considered all time windows of dFCs as a unified entity or treated each time window equally. Actually, the trustworthiness varies for each window due to the inconsistent data quality across different windows, leading to the uncertainty generated from the ensemble information of multiple windows [9]. Unfortunately, current methods ignore this uncertainty arising from the inconsistent data quality, resulting in an inability to evaluate the trustworthiness of different windows.

In this paper, we propose quality-aware fuzzy min-max neural networks (QFMMNet) for dynamic brain network analysis, as shown in Figure 1. In the proposed method, we treat each time window of dFCs as a view and utilize edge-to-edge (E2E), edge-to-node (E2N), and node-to-graph (N2G) convolution filters to extract features of multiple views to obtain evidence [11]. The evidence serves as the input pattern for multi-view fuzzy min-max neural networks (MFMM) to generate hyperboxes, which output class nodes for different views. Our model effectively deals with the fuzzy information in individual views of dFCs, benefiting from the advantages of MFMM in addressing uncertainty and fuzziness. In addition, a quality-aware ensemble module is designed to deal with the uncertainty from different views with inconsistent data quality by identifying the trustworthiness of each view. D-S theory is utilized to directly model uncertainty for multiple views, enabling a more effective assessment of the quality of each view. The information of multiple views is ensembled using a weighted fusion strategy for classification at the decision layer of deep multi-view classification.

2 Proposed Method

2.1 Data and Preprocessing

We utilize raw rs-fMRI data from two schizophrenia datasets. The dataset of Huaxi Hospital (Huaxi) includes 161 patients with schizophrenia and 150 normal control patients (NC). The Center for Biomedical Research Excellence dataset (COBRE) includes 53 patients and 67 NCs. Initial rs-fMRI images are corrected for slice timing, realigned, and normalized to the EPI template. The time-series data are then band-pass filtered (0.01-0.08 Hz). The resulting volumes comprise 240 time points and are segmented into 90 Regions of Interest (ROIs) based on the Automated Anatomical Labeling (AAL) atlas. These time-series provide information about brain activity. The Huaxi dataset retains 9 time windows, resulting in 9 views, while the COBRE dataset retains 10 views.

For a dynamic brain network dataset $\{\mathrm{X}_n\}_{n=1}^{N}$ with N samples, each sample has V windows. Let $A \in \mathbb{R}^{|\Omega| \times |\Omega|}$ be the single adjacency matrix of FCs, i.e., $A^d = \{A(1), A(2), \cdots, A(V)\}$ is the connection matrix of dFCs, where $\Omega = 90$ is the number of brain network nodes.

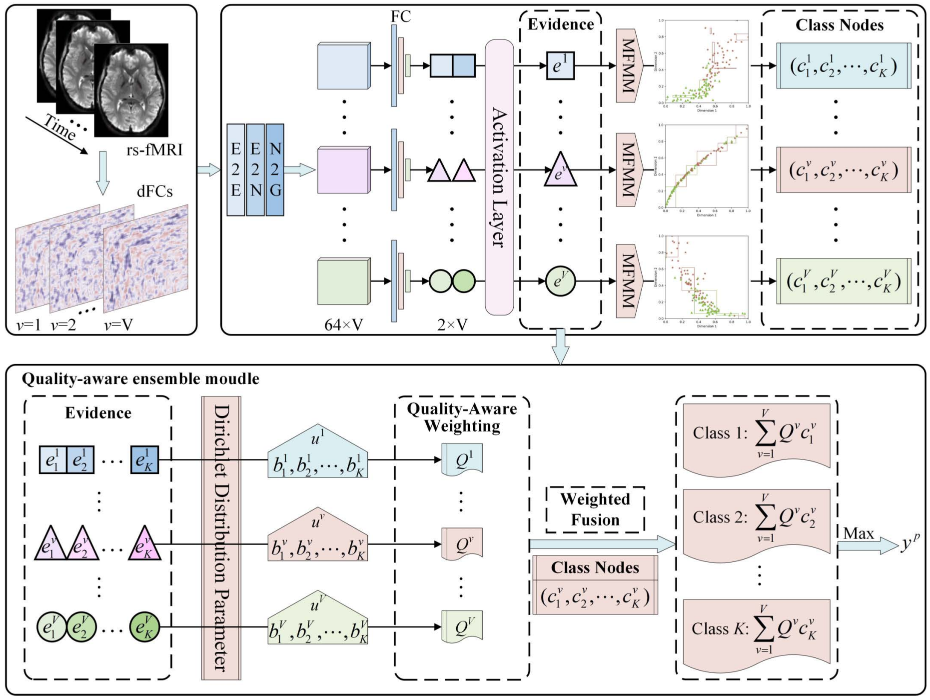

Fig. 1. Evidence is the input pattern of MFMM to obtain the class nodes. The quality-aware ensemble module connects evidence with Dirichlet distribution to evaluate quality-aware weighting and integrates multiple views with weighted fusion.

2.2 Multi-View Fuzzy Min-Max Neural Networks

We design the MFMM to deal with the fuzzy information of dFCs. The MFMM utilizes evidence as input patterns to generate fuzzy hyperboxes, obtaining class nodes under the framework of multi-view learning. To capture multi-view features of brain networks and obtain evidence, we introduce the E2E, E2N, and N2G convolution filters. The details of these filters are as follows:

The E2E extracts edge features from the original adjacency matrix and combines local information weighted to learn edge features. E2E can be defined as

$$H_{i,j}^{(p)}(v) = ReLU(\sum\nolimits_{o=1}^{|\Omega|} (r_o^n A_{i,o}^d(v) + c_o^n A_{o,j}^d(v)) + b^p), \tag{1}$$

where $r^p \in \mathbb{R}^{|\Omega|}$ and $c^p \in \mathbb{R}^{|\Omega|}$ are the learning weights, and b^p is the learning biases of the p-th filter.

The E2N aggregates edge features into node features. E2N can be defined as

$$a_i^{(p)}(v) = ReLU(\sum\nolimits_{m=1}^{M} \sum\nolimits_{o=1}^{|\Omega|} r_o^{m,p} H_{i,o}^m(v) + b^p), \tag{2}$$

where $r_o^{m,p} = \mathbb{R}^{|\Omega|}$ is the learning weight, and (m, p) represents a pair of input and output features for each layer.

The N2G transforms node features into graph features. It reduces the spatial dimension of the feature map by obtaining a single response from all nodes in the graph. N2G can be defined as

$$g^{(p)}(v) = ReLU(\sum_{m=1}^{M} \sum_{i=1}^{|\Omega|} w_i^{m,p} a_i^m(v) + b^p), \tag{3}$$

where $w_i^{m,p} \in \mathbb{R}^{|\Omega|}$ is the learning weight.

The E2E, N2N, and N2G convolution filters are utilized to convolve $\{\mathrm{X}_n\}_{n=1}^N$, producing a feature map $dFC \in \{\{(R_v^{64})_n\}_{v=1}^V\}_{n=1}^N$. The dFC is processed through fully connected layers, followed by a Softplus activation layer, to obtain evidence $e = \{e_1^v, e_2^v, \cdots, e_K^v\}_{v=1}^V$ of each sample for a K classification task.

Fuzzy sets were introduced to deal with the fuzziness, demonstrating high efficiency in pattern recognition problems [21]. We design the MFMM to generate hyperboxes based on fuzzy sets, where the evidence e^v from each view serves as the input pattern. Each hyperbox is represented by a minimum and maximum point in an x-dimensional space within a unit hypercube I^x. Each hyperbox fuzzy set is defined as $HB_j^v = (\{E_n^v, BV_j^v, BW_j^v, h((E_n^v, BV_j^v, BW_j^v))\}), \forall E_n^v \in (I^x)^v$, where HB_j^v is hyperbox fuzzy set of v-th view, $E_n^v = ((e^v)_{n1}, (e^v)_{n2}, \cdots, (e^v)_{nx})$ is the input pattern of v-th view, BV_j^v and BW_j^v are the minimum and maximum points of HB_j^v of the j-th hyperbox.

The MFMM utilizes the membership function to determine the degree of match between the sample and the existing hyperboxes when a new training pattern is provided. The membership function of v-th view is as follows:

$$\begin{aligned} HB_j^v(E_n^v) = \tfrac{1}{2x} \textstyle\sum_{i=1}^{x} [&\max(0, 1 - \max(0, \min(1, e_{ni}^v - BW_{ji}^v))) \\ &+ \max(0, 1 - \max(0, \min(1, BV_{ji}^v - e_{ni}^v)))]. \end{aligned} \tag{4}$$

Hyperbox expansion, hyperbox overlap test, and hyperbox contraction are the main steps of MFMM. The performance may be compromised due to the overlapping regions of hyperboxes from different classes during hyperbox expansion. A new constraint for multi-view data is introduced to solve this problem:

$$\mathrm{Max}_x(BW_{ji}^v, (e^v)_{ni}) - \mathrm{Min}_x(BV_{ji}^v, (e^v)_{ni}) \leq \Theta. \tag{5}$$

Each dimension is examined to confirm whether it exceeds the expansion coefficient Θ in each view, minimizing the overlapping regions of hyperboxes. The reduction of overlapping regions enhances the clarity of decision boundaries, thereby dealing with the fuzzy information.

We employ nine cases as hyperbox overlap test rules to identify all overlapping regions of hyperboxes of different classes. The contraction rules are developed based on the nine cases of the hyperbox overlap test. All cases are examined to determine a proper adjustment. The hyperbox overlap test rules and the hyperbox contraction rules are shown in the **supplementary material**.

2.3 Quality-Aware Ensemble Module

The quality-aware ensemble module was introduced to deal with the uncertainty arising from the inconsistent data quality across each view. We model the uncertainty using the D-S theory and define the dynamic quality-aware weighting to evaluate the quality of each view. The MFMM classifier $f^v(e^v)$ for the v-th view is ensembled by a weighted fusion strategy.

The D-S theory is employed to model uncertainty. For the K classification problems, subjective logic [10] assigns an uncertainty mass to each view based on evidence $e = \{e_1^v, e_2^v, \cdots, e_K^v\}_{v=1}^V$, and assigns a belief mass for each class. The uncertainty mass values and belief mass values are non-negative. The sum of an uncertainty mass value and K belief mass values equals 1 in the v-th view:

$$u^v + \sum\nolimits_{k=1}^{K} b_k^v = 1, \tag{6}$$

where $u^v \geq 0$ is uncertainty mass in the v-th view, and $b_k^v \geq 0$ is belief mass [17].

The Dirichlet distribution is a multidimensional probability distribution used to represent the weight allocation of random variables with multiple categories [20]. Subjective logic relates evidence $e^v = [e_1^v, e_2^v, \cdots, e_K^v]$ to Dirichlet distribution parameters $\alpha^v = [\alpha_1^v, \alpha_2^v, \cdots\cdots, \alpha_K^v]$ in the v-th view by $\alpha_k^v = e_k^v + 1$.

The formulas for belief mass b_k^v and uncertainty u^v are as follows:

$$b_k^v = \frac{e_k^v}{S^v} = \frac{\alpha_k^v - 1}{S^v}, u^v = \frac{K}{S^v}, \tag{7}$$

where $S^v = \sum_{i=1}^{K} (e_i^v + 1) = \sum_{i=1}^{K} \alpha_i^v$ represents the Dirichlet strength.

Definition 1. *Dynamic quality-aware weighting is designed to evaluate the trustworthiness of each view based on uncertainty u^v and belief b_k^v, defined as*

$$Q^v = -\frac{V \log u^v}{\sum_{v=1}^{V} u^v} e^{\mathrm{Max}\{b_1^v, b_2^v, \cdots, b_K^v\}}. \tag{8}$$

The dynamic quality-aware weighting assigns quality-aware weights to the classification results for each view. It is worth noting that the weights for each sample are different, i.e., the weights are dynamically generated.

Definition 1 reveals the pattern that the less the uncertainty mass u^v for the v-th view, the more reliable the classifier $f^v(e^v)$, resulting in higher quality-aware weighting Q^v. We employ a weighted fusion strategy to integrate the classification results of each view at the decision level:

$$f(e) = \sum\nolimits_{v=1}^{V} f^v(e^v) \cdot Q^v. \tag{9}$$

For a sample in $\{\mathrm{X}_n\}_{n=1}^N$ with evidence $e = \{e_1^v, e_2^v, \cdots, e_K^v\}_{v=1}^V$, classification result of v-th view $f^v(e^v) = (c_1^v, c_2^v, \cdots, c_K^v)$ choose the class node with the highest value as the predicted class, i.e., the prediction result of v-th view can be expressed as $(y^p)^v = \mathrm{Max}\{c_1^v, c_2^v, \cdots, c_K^v\}$. The final prediction result of the proposed method for this sample is as follows:

$$y^p = \mathrm{Max}\left\{\sum\nolimits_{v=1}^{V} Q^v c_1^v, \sum\nolimits_{v=1}^{V} Q^v c_2^v, \cdots, \sum\nolimits_{v=1}^{V} Q^v c_K^v\right\}. \tag{10}$$

2.4 Network Structure and Training

The cross-entropy loss $\ell_{ce} = -\sum_{k=1}^{K} y_{nk} \log(p_{nk})$ is the commonly used loss function in the context of traditional neural network classifiers, where p_{nk} is the predicted probability of class k for the n-th sample.

For the proposed model, we can derive the Dirichlet distribution parameters α_n from the evidence learned for the n-th sample. Parameters α_n are then utilized to generate multinomial opinions denoted as $Dir(P_n|\alpha_n)$, where P_n represents the probability distribution for category assignments on the simplex. We make modifications to the cross-entropy loss function ℓ_{ce}:

$$\ell_{ace}(\alpha_n) = \sum_{k=1}^{K} y_{nk}(\psi(S_n) - \psi(\alpha_{nk})), \tag{11}$$

where $\psi(\cdot)$ is the digamma function. The loss function ℓ_{ace} allows the model to produce more evidence of the correct class during training. Additionally, we introduce a KL divergence term to add a prior to the Dirichlet distribution as a regularization term, aiming to reduce evidence for incorrect classes:

$$\ell_{kl}^{v}(\alpha^v) = D_{KL}[Dir(P^v|\tilde{\alpha}^v)||Dir(P^v|[1, \cdots, 1])], \tag{12}$$

where $\tilde{\alpha}^v = y + (1 - y) \odot \alpha^v$ is the adjustment parameter for the Dirichlet distribution, preventing the penalization of evidence for the correct class to 0.

For the n-th sample with Dirichlet distribution parameters α_n, the optimized loss function for the v-th view is defined as follows:

$$\ell_n^v = \ell_{ace}(\alpha_n^v) + \lambda \ell_{kl}^v(\alpha_n^v), \tag{13}$$

where $\lambda > 0$ is the balancing factor. Overemphasizing KL divergence in the early stages of training may lead to the loss of crucial information. Thus, we increase the value for λ steadily. By minimizing the overall loss function

$$\ell = \sum_{n=1}^{N} \sum_{v=1}^{V} \ell_n^v, \tag{14}$$

all views are ensured to improve the overall opinion.

3 Experiments

3.1 Experimental settings

The classification performance of the proposed model QFMMNet is evaluated by measuring accuracy (ACC), sensitivity (SEN), specificity (SPE), and F1-score ($F1$) via 5-cross validation.

We compared our model with 2 classification algorithms based on hyperbox, including enhanced fuzzy min-max neural networks (EFMM) [14], and general fuzzy min-max neural networks (GFMM) [12]. We also compared our model with 3 deep multi-view algorithms, including a multi-omics integration-based biomedical data classifier (MORONET) [18], trusted multi-view classification (TMC) [7], and a dynamic fusion-based trustworthy multi-modal classifier (MMD) [6]. Furthermore, we conducted ablation studies using only MFMM (NoQAE) and quality-aware ensemble module (NoMFMM), respectively.

Table 1. Performance Comparison of the Proposed and Competing Methods.

Datasets	Methods	ACC(%)	SEN(%)	SPE(%)	F1(%)
Huaxi	EFMM	80.71 ± 1.03	78.51 ± 2.76	82.61 ± 2.71	79.48 ± 2.84
	GFMM	82.32 ± 1.02	80.33 ± 1.28	84.26 ± 1.34	82.12 ± 1.55
	MORONET	73.39 ± 1.42	64.53 ± 3.38	81.48 ± 3.55	70.30 ± 2.05
	TMC	83.93 ± 2.63	83.05 ± 3.31	84.43 ± 3.38	83.06 ± 3.71
	MMD	83.66 ± 2.31	82.71 ± 2.63	84.81 ± 4.04	83.38 ± 2.88
	NoQAE	82.63 ± 1.26	80.96 ± 4.47	83.65 ± 3.69	81.54 ± 3.14
	NoMFMM	83.60 ± 2.15	82.25 ± 4.29	84.36 ± 2.90	82.56 ± 3.90
	Ours	**87.14 ± 1.40**	**88.60 ± 1.97**	**85.61 ± 2.80**	**88.03 ± 1.27**
COBRE	EFMM	82.50 ± 1.66	85.14 ± 4.46	79.00 ± 2.59	84.12 ± 2.84
	GFMM	83.33 ± 2.63	87.55 ± 4.93	76.39 ± 6.73	85.07 ± 3.60
	MORONET	81.67 ± 2.04	88.68 ± 3.11	71.97 ± 2.79	84.86 ± 2.04
	TMC	83.33 ± 2.63	89.52 ± 4.04	75.00 ± 3.52	85.69 ± 3.04
	MMD	83.81 ± 1.91	88.75 ± 3.50	77.38 ± 1.23	85.74 ± 2.77
	NoQAE	83.81 ± 0.95	87.05 ± 4.58	79.16 ± 4.36	85.00 ± 2.74
	NoMFMM	82.50 ± 3.21	88.68 ± 3.94	73.26 ± 7.62	85.66 ± 3.56
	Ours	**87.50 ± 2.64**	**91.01 ± 3.88**	**82.17 ± 4.43**	**89.07 ± 3.30**

3.2 Results

Experimental results are listed in Table 1, indicating that our model consistently outperforms others across all metrics and exhibits superior classification performance compared to other methods. For instance, the ACC reached 87.14% and 87.50% on Huaxi and COBRE, showing significant improvement. The ablation studies proved the effectiveness of MFMM and quality-aware ensemble module.

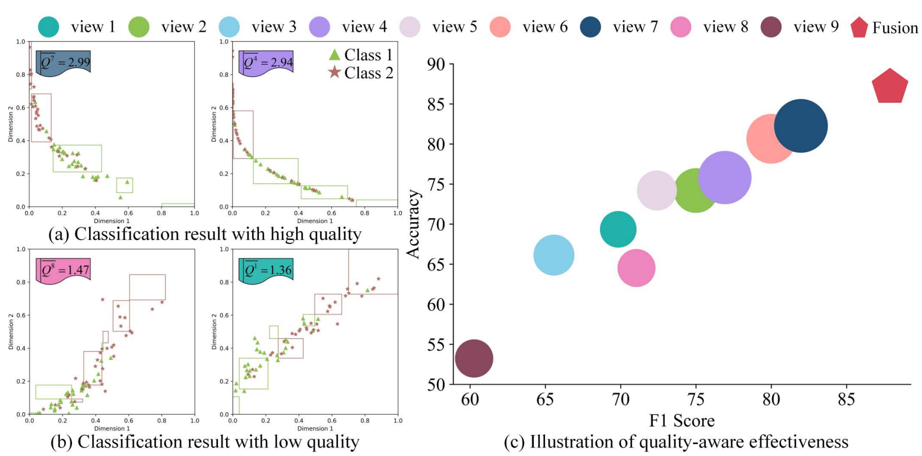

Fig. 2. Classification results of MFMM with high (a) and low (b) quality. The size of the points (c) is associated with the average dynamic quality-aware weight $\overline{Q^v}$ of all samples, and the larger points correspond to higher quality, and vice versa.

We utilized ACC and $F1$ as evaluation metrics to verify the effectiveness of our model in dealing with fuzzy information and uncertainty. Figure 2 illustrates the phenomenon wherein points closer to the upper-right corner indicate better classification results. The phenomenon proves that our model can identify the quality of views and effectively ensemble multiple views, thereby enhancing the trustworthiness of classification.

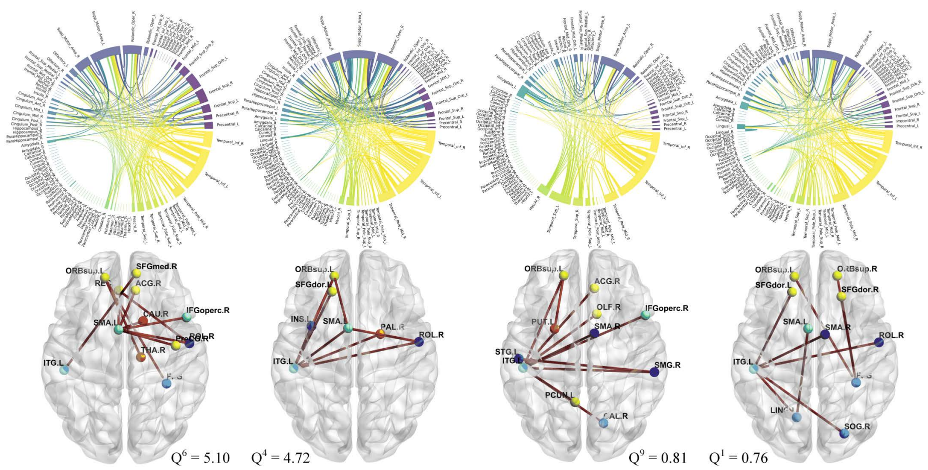

(a) Discriminant connections with high quality (b) Discriminant connections with low quality

Fig. 3. The first row shows the discriminative connections, and the second row illustrates the map of the brain regions corresponding to the strongest connections.

3.3 Maps of Discriminative Connections

Our proposed model can identify discriminative connections based on backpropagated gradient information. As shown in Figure 3, all views have captured discriminative brain regions associated with the disease (e.g., ITG.L and ORBsup.L). Furthermore, high-quality views predominantly involve brain regions in the frontal lobe, which is closely related to schizophrenia. While a more dispersed pattern is observed in low-quality views, affecting the decision.

4 Conclusion

We propose a novel dynamic brain network analysis method based on quality-aware fuzzy min-max neural networks (QFMMNet). Our model employs the multi-view fuzzy min-max neural networks (MFMM) based on fuzzy sets to deal with the fuzzy information of dFCs. A quality-aware ensemble module is designed to deal with the uncertainty arising from the inconsistent data quality of different windows, improving the trustworthiness of the decision. Experimental results on Huaxi and COBRE datasets demonstrate the efficacy of our method.

Acknowledgments. This study was funded by the National Natural Science Foundation of China (61976120, 62102199, 62371261), the Natural Science Foundation of Jiangsu Province (BK20231337), the Natural Science Key Foundation of Jiangsu Education Department (21KJA510004), the China Postdoctoral Science Foundation (2022M711716), the General Program of the Natural Science Research of Higher Education of Jiangsu Province (23KJB520031), the Postgraduate Research & Practice Innovation Program of Jiangsu Province (SJCX23_1781).

Disclosure of Interests. The authors have no competing interests to declare that are relevant to the content of this article.

References

1. Bijsterbosch, J., Harrison, S.J., Jbabdi, S., Woolrich, M., Beckmann, C., Smith, S., Duff, E.P.: Challenges and future directions for representations of functional brain organization. Nature Neuroscience **23**(12), 1484–1495 (2020)
2. Bolton, T.A., Morgenroth, E., Preti, M.G., Van De Ville, D.: Tapping into multi-faceted human behavior and psychopathology using fmri brain dynamics. Trends in Neurosciences **43**(9), 667–680 (2020)
3. Caballero-Gaudes, C., Reynolds, R.C.: Methods for cleaning the bold fmri signal. Neuroimage **154**, 128–149 (2017)
4. Chen, J.E., Polimeni, J.R., Bollmann, S., Glover, G.H.: On the analysis of rapidly sampled fmri data. Neuroimage **188**, 807–820 (2019)
5. Fiorenzato, E., Strafella, A.P., Kim, J., Schifano, R., Weis, L., Antonini, A., Biundo, R.: Dynamic functional connectivity changes associated with dementia in parkinson's disease. Brain **142**(9), 2860–2872 (2019)
6. Han, Z., Yang, F., Huang, J., Zhang, C., Yao, J.: Multimodal dynamics: Dynamical fusion for trustworthy multimodal classification. In: Proceedings of the IEEE/CVF Conference on Computer Vision and Pattern Recognition. pp. 20707–20717. IEEE (2022)
7. Han, Z., Zhang, C., Fu, H., Zhou, J.T.: Trusted multi-view classification with dynamic evidential fusion. IEEE Transactions on Pattern Analysis and Machine Intelligence **45**(2), 2551–2566 (2022)
8. Huang, J., Wang, M., Ju, H., Shi, Z., Ding, W., Zhang, D.: Sd-cnn: A static-dynamic convolutional neural network for functional brain networks. Medical Image Analysis **83**, 102679 (2023)
9. Hutchison, R.M., Womelsdorf, T., Allen, E.A., Bandettini, P.A., Calhoun, V.D., Corbetta, M., Della Penna, S., Duyn, J.H., Glover, G.H., Gonzalez-Castillo, J., Handwerker, D.A., Keilholz, S., Kiviniemi, V., Leopold, D.A., de Pasquale, F., Sporns, O., Walter, M., Chang, C.: Dynamic functional connectivity: promise, issues, and interpretations. Neuroimage **80**, 360–378 (2013)
10. Jøsang, A., Hankin, R.: Interpretation and fusion of hyper opinions in subjective logic. In: 2012 15th International Conference on Information Fusion. pp. 1225–1232. IEEE (2012)
11. Kawahara, J., Brown, C.J., Miller, S.P., Booth, B.G., Chau, V., Grunau, R.E., Zwicker, J.G., Hamarneh, G.: Brainnetcnn: Convolutional neural networks for brain networks; towards predicting neurodevelopment. NeuroImage **146**, 1038–1049 (2017)
12. Khuat, T.T., Gabrys, B.: Accelerated learning algorithms of general fuzzy min-max neural network using a novel hyperbox selection rule. Information Sciences **547**, 887–909 (2021)
13. Liu, M., Zhang, H., Shi, F., Shen, D.: Building dynamic hierarchical brain networks and capturing transient meta-states for early mild cognitive impairment diagnosis. In: Medical Image Computing and Computer Assisted Intervention – MICCAI 2021. pp. 574–583. Springer (2021)
14. Mohammed, M.F., Lim, C.P.: An enhanced fuzzy min–max neural network for pattern classification. IEEE Transactions on Neural Networks and Learning Systems **26**(3), 417–429 (2015)
15. Park, H.J., Friston, K.: Structural and functional brain networks: from connections to cognition. Science **342**(6158), 1238411 (2013)

16. Park, J., Hwang, Y., Kim, M., Chung, M.K., Wu, G., Kim, W.H.: Convolving directed graph edges via hodge laplacian for brain network analysis. In: Medical Image Computing and Computer Assisted Intervention – MICCAI 2023. pp. 789–799. Springer (2023)
17. Wang, H., Subramanian, V., Syeda-Mahmood, T.: Modeling uncertainty in multimodal fusion for lung cancer survival analysis. In: 2021 IEEE 18th international symposium on biomedical imaging (ISBI). pp. 1169–1172. IEEE (2021)
18. Wang, T., Shao, W., Huang, Z., Tang, H., Zhang, J., Ding, Z., Huang, K.: Mogonet integrates multi-omics data using graph convolutional networks allowing patient classification and biomarker identification. Nature Communications **12**(1), 3445 (2021)
19. Wen, Z., Seo, J., Pace-Schott, E.F., Milad, M.R.: Abnormal dynamic functional connectivity during fear extinction learning in ptsd and anxiety disorders. Molecular Psychiatry **27**(4), 2216–2224 (2022)
20. Wong, T.T.: Generalized dirichlet distribution in bayesian analysis. Applied Mathematics and Computation **97**(2-3), 165–181 (1998)
21. Zadeh, L.A.: Fuzzy sets. Information and Control **8**(3), 338–353 (1965)
22. Zhu, Q., Xu, R., Wang, R., Xu, X., Zhang, Z., Zhang, D.: Stacked topological preserving dynamic brain networks representation and classification. IEEE Transactions on Medical Imaging **41**(11), 3473–3484 (2022)